

Corona-induced micro-centrifugal flows for concentration of *Neisseria* and *Salmonella* bacteria prior to their quantitation using antibody-functionalized SERS-reporter nanobeads

Yuan-Yu Chen¹ · Yu-Cheng Fang¹ · Shih-Yun Lin¹ · Yi-Jyun Lin¹ ·
Shih-Ying Yen¹ · Chen-Han Huang² · Chiou-Ying Yang³ · Lai-Kwan Chau^{1,2} ·
Shau-Chun Wang^{1,2}

Received: 1 August 2016 / Accepted: 7 January 2017 / Published online: 2 February 2017
© Springer-Verlag Wien 2017

Abstract The use of microcentrifugal flows driven by ionic wind that is generated near a corona needle tip above the level of a small liquid reservoir is a technique to trap suspended bacteria within a few minutes. Gas ions are ejected at the tip of a corona needle to form an ionic wind that can swipe across the liquid/air interface inside a miniaturized reservoir to generate centrifugal vortices. This will drag suspended particles to the center of the reservoir. This article describes a method where antigen-functionalized polystyrene microspheres are first employed to mimic bacteria. The mimetic bacteria were then detected by surface-enhanced Raman scattering (SERS) signal after binding antibody-conjugated nanoaggregate-embedded beads (NAEBs) to antigen-functionalized polystyrene microspheres. The NAEBs were prepared from silica-coated gold nanoparticle aggregates and labeled with Raman reporter

molecules. The work demonstrates that the particles can be concentrated at the stagnant point at the bottom of a reservoir containing 60 μL solution only by ionic wind-driven centrifugal flows. SERS signals were acquired to identify the bacteria-mimicking particles. The ionic wind flows were then applied to trap and concentrate *Neisseria* and *Salmonella* bacteria bound with antibody-conjugated NAEBs at the level of 10^6 colony forming units (CFU) per mL (or lower) within 10 min. The NAEBs were preferably labeled with Ethyl violet or fluorescein derivatives. The log-log calibration plot for *Neisseria* is linear in the 10^4 to 10^6 CFU·mL⁻¹ concentration range.

Keywords Microfluidics · Vortex flow · Microcentrifuge · Ionic wind · Raman tag · Bacteria detection · SERS · *Neisseria* · *Salmonella* · Immunoassay

Electronic supplementary material The online version of this article (doi:10.1007/s00604-017-2077-7) contains supplementary material, which is available to authorized users.

- ✉ Chiou-Ying Yang
cyang@dragon.nchu.edu.tw
- ✉ Lai-Kwan Chau
chelkc@ccu.edu.tw
- ✉ Shau-Chun Wang
chescw@ccu.edu.tw

- ¹ Department of Chemistry and Biochemistry, National Chung Cheng University, Chia-Yi 621, Taiwan
- ² Center for Nano Bio-Detection, AIM-HI, National Chung Cheng University, Chia-Yi 621, Taiwan
- ³ Institute of Molecular Biology, National Chung Hsing University, Taichung 402, Taiwan

Introduction

Conventional methods of analyzing pathogenic bacteria are time-consuming because of bacterial counts as low as 10^3 colony forming units (CFU) mL⁻¹ can be found in biological samples from living sources. Although rapid methods such as polymerase chain reaction and nucleic acid probes are more sensitive and selective than conventional techniques, many of these tests are compromised by complicated matrix components [1].

Therefore sample culturing is needed to increase the bacteria concentration at least by 1000-fold. Slow bacteria cultivation procedures can take anywhere from 24 h to weeks to accomplish. Alternative methods are in demand to rapidly separate and concentrate bacteria directly from samples, thereby minimizing the assay time.

An impedance spectroscopy method was used to detect specific bacteria bound with antibody-immobilized gold nanoparticles to reach LOD of 30 CFU·mL⁻¹. Unfortunately, simultaneous detection of different bacteria was not possible using this method [2]. To allow multiplexing capability, various functionalized nanoparticles have been used to develop bacteria detection techniques for providing adequate sensitivity. Based on the competitive bindings of cationic polymer-coated gold nanoparticles to the enzyme and bacteria, a highly sensitive colorimetric assay was developed [3]. Although the limit of detection (LOD) at 10 CFU·mL⁻¹ is impressive, this method lacks selectivity.

Other immunoassays using fluorescent quantum dot (QD) tagged carbon nanoparticles show adequate simultaneous detection of different kinds of bacteria with LOD lower than 100 CFU·mL⁻¹ [4, 5]. However, because fluorescence emission peaks were broad, multiplex detection capability of these assays were limited to two or three bacteria species. Furthermore, functionalized magnetic nanoparticles have been used to bind with bacteria to concentrate prior to conjugating with QD nanoparticles for detection. Nevertheless, the tedious assay development procedures to optimize the amounts of magnetic nanoparticles and QD nanoparticles are time consuming [6].

To address the aforementioned technical difficulties, miniaturized diagnostic systems for analyzing pathogen bacteria have been widely studied over the last ten years [7, 8]. The contribution of chip-based device for diagnostics is the removal of the bottleneck in sample culturing time by trapping and concentrating the bacteria in the original sample at one location to dramatically increase detection sensitivity.

Current on-chip enrichment methods often use AC dielectrophoresis (DEP) related technologies to direct and concentrate the bacteria [9]. Successful integrations of SERS detection with DEP microfluidic platform to recognize bacteria have been reported [10–12]. The DEP mechanism is based on the polarization of a particle in a nonuniform electric field, to be attracted to an area of which the field strength is higher or lower than that of other locations, depending upon the particle polarizability relative to the medium [13]. However, the force acting on the particle DEP scale as a^3 where a is the particle radius. As a result, the particle velocity is proportional to a^2 . Therefore, micron-size bacteria would only be concentrated on an electrode by DEP when they are near the electrode surface.

Alternatively, electrophoretic forces were also used to drive bacteria into designate region to concentrate [14–17]. The adequate dragging force to sufficiently move bacteria can be generated only under high field strength (~ 1 kV·cm⁻¹), which usually damages the bacteria cell membranes and causes severe chemical contaminations due to electrode reactions.

When a needle electrode, applied with a high AC voltage (≥ 1 kV) of high frequency (≥ 50 kHz), hanging ~ 3 mm above

the surface of an electrically grounded small reservoir, plasma ions buildup on the electrode tip are then propelled away from the localized ionization region along the field lines in the direction of decreasing field intensity. Consequently, these plasma ions collide with electroneutral air molecules to generate a gas stream known as ionic wind [18]. Finally, the momentum due to these collisions imparts onto the liquid interface. In addition, because of tangential shear at the air-liquid interface, intense surface vortices with linear velocities in excess of 1 cm/s can be obtained. When the electrode is placed off-center, only one dominant vortex is observed in the reservoir to generate a centrifugal flow to trap microspheres to the stagnant point at the reservoir bottom to accomplish particle concentration within minutes [18, 19].

Raman spectroscopy is another popular bioanalytical tool [20]. The chemical structures with specific functionalities modulate the frequency shifts of scattering light to corresponding frequencies. Therefore, this spectroscopic technique can obtain the fingerprint signature signals of various moieties to identify molecular structures. Unlike IR spectroscopy, which measures the light absorbance caused by the vibrational frequencies of functional groups, is prone to solvent background interferences, Raman spectroscopy is particularly useful to determine analytes in aqueous solution due to its limited background signals of water.

Although Raman scattering signals are very weak, signal enhancement techniques using nanoparticles or the rough structures of noble metals to amplify localized electromagnetic fields of probing light beam, known as surface enhanced Raman scattering (SERS), have significantly improved the Raman scattering signal intensities. In particular, SERS detections have been successfully used in environmental pollutant determinations and biomedical applications [21, 22]. Besides, SERS techniques can characterize bacteria by identifying the specific proteins, amino acids, and sugars on the cell surfaces [23–25]. However, the intensities of signature SERS signal peaks of moieties on the surfaces of different bacteria sometimes significantly vary. Thus, simultaneous recognitions of various bacteria are problematic when the signal peaks of some bacteria with weaker SERS scattering intensities are buried in the signals of others with stronger intensities.

Alternatively, using specially designed surface-enhanced Raman scattering (SERS) nanoprobe, such as nanoaggregate embedded beads (NAEBs) conjugated with specific antibody, have been reported to detect various kinds of bacteria simultaneously [26, 27]. The NAEB is a stable colloid prepared through controlled aggregation of a few gold nanoparticles (AuNPs) encapsulated together with SERS reporters in a protective silica shell [26–29]. Conjugated with a specific antibody, each NAEB can serve as a highly sensitive SERS active nanosensor to probe the target analyte, such as bacteria. The Raman tag presents as a particular SERS identification barcode of narrow Raman peaks via excitation.

Here we report the use of Raman reporter-labeled NAEBs, conjugating with specific antibody probes, to recognize and quantify *Neisseria* and *Salmonella* bacteria in a small reservoir at the level of 10^6 CFU mL⁻¹ or lower. The high voltage needle above the reservoir solution level generates ionic wind vortex flows to trap NAEBs-bound bacteria around the center of reservoir bottom without using any other capturing units. The concentrated bacteria of *Neisseria* and *Salmonella* can be clearly identified using the spectrum features of SERS reporters in each kind of NAEB, of which the signal intensities are comparable. The bacteria concentrations can also be quantified using SERS signal peak intensities.

Experimental

Materials

Indium titanium oxide (ITO) coated conducting glass slides of 0.07 cm in thickness and 7.5 cm × 2.5 cm in area, which were purchased from Uni-Onward Corp. (Taipei, Taiwan, www.uni-onward.com.tw), were used as chip substrate. Vivak® copolyester plastic sheet (0.5 cm in thickness) was obtained from DSM Engineering Plastic Products (Sheffield, MA, www.dsm.com) to fabricate chip slide in the same area size as that of ITO glass slide.

The following chemical and biochemical reagents were used as received. Hydrogen tetrachloroaurate trihydrate (HAuCl₄ · 3H₂O; 99.9%) and sodium citrate tribasic dihydrate (99%) were obtained from Showa (www.showa1.com) to synthesize AuNPs.

Silica-based shells to encapsulate gold nanoparticles and Raman reporters as NAEB tags were prepared using tetraethylorthosilicate (TEOS; 99.0%) and (3-aminopropyl) triethoxysilane (APTES; 99%) from Sigma-Aldrich (www.sigmaaldrich.com), and (3-mercaptopropyl)-trimethoxysilane (MPTMS; 95%; ACROS, www.acros.com). Basic solutions were prepared with sodium hydroxide (97%, Showa, www.showa1.com) and ammonium hydroxide (28.0–30.0 wt.% in water; Sigma-Aldrich, www.sigmaaldrich.com). Anhydrous ethanol (TEDIA) was used as rinsing solvent in preparation procedures. The Raman reporter molecules tagged in NAEB's were as follows: ethyl violet (EV) and tetramethylrhodamine-5-isothiocyanate (TRITC) from Sigma-Aldrich (www.sigmaaldrich.com), and malachite green isothiocyanate (MGITC) from Thermo Fisher Scientific (www.thermofisher.com).

Prior to functionalization of polystyrene microspheres with an antigen, N-hydroxysuccinimide (98%; NHS) and N-(3-dimethylaminopropyl)-N'-ethylcarbodiimide hydrochloride (EDC; 99.0%) obtained from Sigma-Aldrich were used to activate the surface of the microspheres. Buffer

solutions used in this surface modification procedures included monopotassium phosphate (99.0%) and disodium hydrogen phosphate (99.0%) from Showa (www.showa1.com), and ethanolamine (99.0%) from Sigma-Aldrich (www.sigmaaldrich.com). Sodium chloride (99.0%, Sigma-Aldrich, www.sigmaaldrich.com) and potassium chloride (99.0%, Showa, www.showa1.com) were used to adjust solution ionic strength.

Polystyrene (PS) carboxylate microspheres (5 μm) were from Polysciences, Inc. (www.polysciences.com). The antigen/antibody pair for binding interaction were ovalbumin (OVA, Sigma-Aldrich, www.sigmaaldrich.com) on PS microspheres and monoclonal anti-ovalbumin antibody (anti-OVA; Sigma-Aldrich, www.sigmaaldrich.com) on NAEBs, respectively. Unless otherwise noted, all solutions were prepared with deionized water (18.2 MΩ·cm) from a Millipore (www.merckmillipore.com) Milli-Q system.

Procedures

Preparations of antibody-conjugated NAEBs

The preparation procedures of conjugating antibody on NAEBs followed the procedures in previous papers [26–29]. Details are described in the [supplementary materials](#) of this paper. In particular, MGITC-labeled NAEBs were conjugated with anti-OVA to recognize OVA-functionalized PS microspheres. TRITC and EV-labeled NAEBs were conjugated with monoclonal antibodies mAb 4B2D and 4–7–3, respectively to recognize targeted bacteria. As described in our previous paper [27], mAbs 4B2D and 4–7–3 are specific for *Salmonella* and *Neisseria*, respectively.

Sample preparations

The protocol of preparing antigen-functionalized PS microspheres followed the procedures in our previous paper [27]. Details are also described in [supplementary materials](#).

In particular, bacteria samples were in phosphate buffer at various cell concentrations ranged from 10^4 to 2×10^6 CFU·mL⁻¹. Each sample was mixed with a solution containing excess amount of antibody-functionalized NAEBs and shook for 1 h for binding. The NAEBs-bound bacteria were sedimentated by centrifuging the solution in a sample tube at 553 ref for 15 min. The free unbound NAEB solution at the upper layer was siphoned out and the remaining NAEBs-bound bacteria in the sample tube were re-dispersed in deionized water. The solution was centrifuged, siphoned, and re-dispersed with water one more time to clean up residue phosphate in bacteria precipitates. These clean-up steps minimize the matrix effects in slowing down vortex flows.

Fabrications of micro-centrifugal device

To fabricate a micro-centrifugal chip, the edges of one copolyester slide (7.5 cm × 2.5 cm), containing a reservoir hole (0.8 cm i.d.) at its center, were melted by acetone to seal with the other ITO coated conducting glass slide with the same size by clamping these two slides with adequate pressure force. The reservoir volume in the chip was 60 μL . Prior to the sealing, one small piece of copper ribbon electrode was taped near the plastic slide edge to serve as an electrical contact to connect with the power source.

Equipment set-up of micro-centrifugal system

As shown in Fig. 1, a functional generator from Agilent Technologies (www.agilent.com) provided the ac output waveform of 50 kHz (0.5–1.0 V), amplified via one broadband amplification system and finally pumped to ~ 1000 V_{rms} with a transformer. Both broadband voltage amplifier and transformer were from Industrial Testing Equipment Co. (Port Washington, NY, www.industrialtest.com). The output voltage was applied on the corona needle of platinum wire (0.5 cm). This wire was hanged 3 mm above the reservoir liquid. One piece of copper ribbon electrode was taped on the chip as the ground end. The platinum needle was inclined at 30-degree angle from the liquid level and off the reservoir center, pointing tangentially near the edge of the circular reservoir. These optimized corona parameters were similar to the conditions used in previous works [18, 19].

The chip was stationed at the stage of one inverted-view microscope (IX51, Olympus Corp., Japan, www.olympus-global.com) equipped with CCD camera (ProgRes®, Jenoptik, Germany, www.jenoptik.com), from which the acquired images were stored in a personal computer.

Using ionic winds to concentrate microparticles and bacteria in micro-centrifugal chip

One aliquot (60 μL) of NAEBs-bound microsphere or bacteria sample was added into the chip reservoir. When the ac voltage is applied, the stream of ionic wind coming from the needle tip generates one vortex to produce centrifugal flows. The suspended PS microspheres and bacteria were dragged into the centrifugal vortex and then trapped at the flow stagnant point near the center of reservoir bottom in 5 to 10 min.

As described in the previous section, the chip was stationed at the stage of one inverted-view microscope to videotape the process of trapping and concentrating functionalized PS microspheres or bacteria bound with NAEBs using a CCD camera storing images in a personal computer.

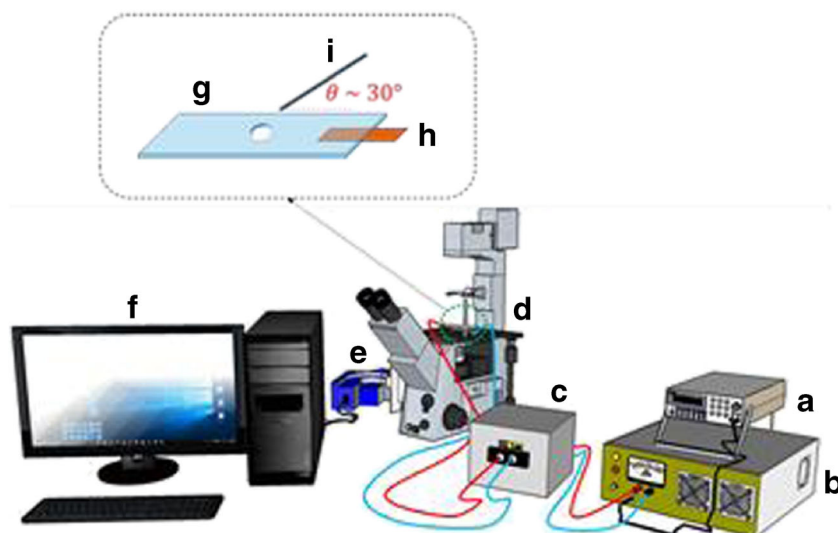
When the NAEBs-bound PS microspheres or bacteria were trapped to accumulate at the center of reservoir bottom, the chip was moved to acquire the Raman spectrum of the reporter molecules in NAEBs from the accumulated spot using micro-Raman spectroscope (XploRA, Horiba Scientific, Japan, www.horiba.com). The wavelength of incident laser was at 638 nm. The Raman spectrum was acquired through a 10X objective.

Results and discussion

Trappings of polystyrene (PS) microspheres bound with NAEBs

As described in Experimental section, the solution containing OVA-functionalized PS microspheres (4.5×10^8 mL⁻¹) was mixed with MGITC-labeled NAEBs, of which the surfaces

Fig. 1 The schematic illustration of experimental set-up for bacteria concentration using corona-induced micro-centrifugal flows. **a.** functional generator; **b.** power amplifier; **c.** transformer; **d.** inverted-view microscope; **e.** CCD camera; **f.** personal computer. The top imbed graph shows the chip **g** containing centrifugal reservoir with one copper ribbon electrode **h** taped between two chip slides. One corona needle **i** inclined at the angle 30° is hanging above the reservoir. The chip is stationed on the microscope stage as indicated in the dashed green circle



were conjugated with anti-OVA for binding. An aliquot containing 60 μL solution of NAEBs-bound PS microspheres was then added into the micro-centrifugal device reservoir. The ionic winds coming from the high voltage needle generates vortex flows to trap these NAEBs-bound PS beads around the center of reservoir bottom in 5 min, as shown in the imbedded graph of Fig. 2. These findings of trapped PS microspheres of 5 μm i.d. were consistent with the observations in the previous paper [19]. The Raman spectrum (trace A) in Fig. 2 was taken at the stagnant point in which the PS microspheres were accumulated. The comparison spectrum was acquired at a non-stagnant point. The featureless Raman spectrum as shown in trace B of Fig. 2 was obtained at the non-stagnant point. Such a spectrum virtually overlaps with that of blank spectrum (trace C) acquired prior to the activation of ionic winds. On the other hand, the characteristic peaks of MGITC at 1170, 1370, and 1620 cm^{-1} , as indicated by red dots in trace A of Fig. 2, are significantly above the blank signals.

This model system verifies the concept of trapping NAEBs-bound PS microspheres and identifying the particles using the Raman spectrum features of reporter molecules in NAEBs, when an antibody is conjugated on the surface of NAEBs to bind with the corresponding antigen-functionalized PS microspheres.

Trapping and identification of *Neisseria* and *Salmonella* bound with antibody-conjugated NAEBs

The solution containing *Neisseria* (1.0×10^6 CFU·mL $^{-1}$) was mixed with TRITC-labeled NAEBs which conjugated

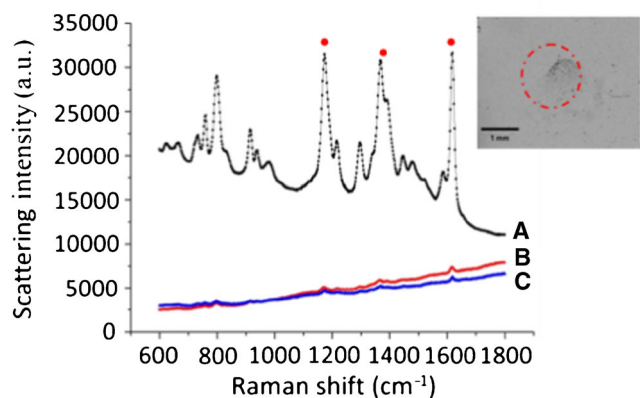


Fig. 2 The Raman scattering spectra acquired under ionic wind vortex flows at **a** the stagnant point, where NAEBs-bound PS microspheres are concentrated, and **b** the non-stagnant point where PS microsphere accumulations were not found. Trace C is the blank spectrum acquired prior to the flow activation. The characteristic peaks of MGITC-labeled NAEBs at 1170, 1370, and 1620 cm^{-1} , are indicated by red dots above trace A. The inset photograph next to the main graph shows the accumulation of PS microspheres (in the dashed red circle) around the center of reservoir bottom

with mAb 4–7–3 antibody. This conjugated antibody possesses highly specific binding affinity with *Neisseria*. An aliquot of NAEBs-bound *Neisseria* solution (60 μL) was then added into the micro-centrifugal device reservoir. The ionic winds coming from the high voltage needle generates vortex flows to trap these bacteria around the center of reservoir bottom within 10 min, as shown in the imbedded graph of Fig. 3. Similarly, *Salmonella* solution (2.0×10^6 CFU·mL $^{-1}$) was mixed with EV-labeled NAEBs which conjugated with mAb 4B2D antibody for binding. Then an aliquot of the resulting NAEBs-bound *Salmonella* solution (60 μL) was added into the device reservoir to concentrate at the stagnant point of ionic wind-driven flows.

Traces A and B in Fig. 3 contain clear SERS spectrum features of EV and TRITC, respectively. Trace A was acquired from *Salmonella* (2.0×10^6 CFU·mL $^{-1}$). Trace B was from *Neisseria* (1.0×10^6 CFU·mL $^{-1}$). These bacteria were trapped at the stagnant point on the reservoir bottom. Trace C is one featureless blank spectrum acquired from a non-stagnant point, showing no

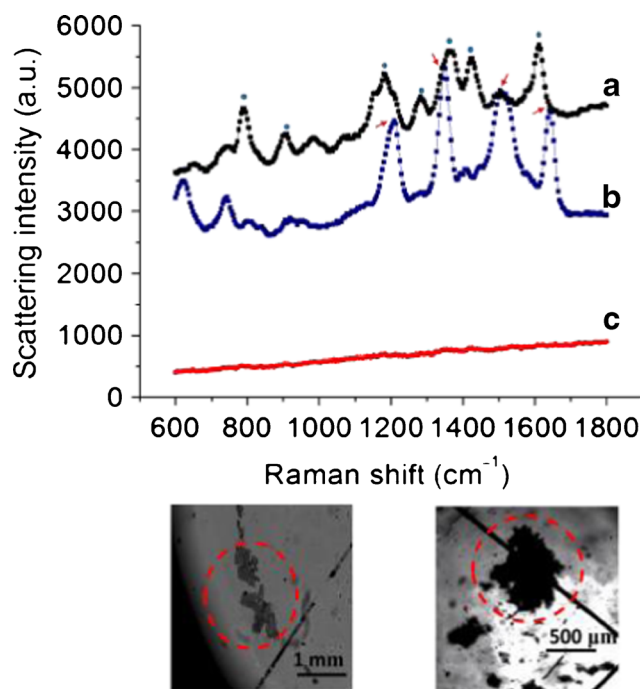


Fig. 3 The Raman scattering spectra acquired under ionic wind vortex flows at the stagnant points, where NAEBs-bound bacteria samples including *Salmonella* (trace A) and *Neisseria* (trace B) of concentrations of 2.0×10^6 and 1.0×10^6 CFU·mL $^{-1}$, respectively, are concentrated. Trace C is the blank spectrum acquired prior to the flow activation. The characteristic peaks of EV-labeled NAEBs at 800, 914, 1200, 1293, 1373, 1428, and 1620 cm^{-1} are indicated by blue dots above trace A. The characteristic peaks of TRITC-labeled NAEBs at 1220, 1360, 1530, and 1650 cm^{-1} are marked by red arrows above trace B. The inset photographs below the main graph show the accumulation of NAEBs-bound *Neisseria* (in the dashed red circle) around the center of reservoir bottom. The left and right images were acquired using 10^4 and 10^6 CFU·mL $^{-1}$ samples, respectively

distinguishable signals. The characteristic Raman scattering peaks of EV appear in trace A at 800, 914, 1200, 1293, 1373, 1428, and 1620 cm^{-1} , respectively. Trace B contains the characteristic Raman scattering peaks of TRITC at 1220, 1360, 1530, and 1650 cm^{-1} . Besides, the signal peaks in traces A and B acquired from NAEBs-bound *Salmonella* and *Neisseria* samples at similar concentrations are in comparable intensities.

The photographs below the main graph show the NAEBs-bound *Neisseria* aggregates precipitated at the reservoir bottom after the centrifuge step. The left image, acquired using 10^4 $\text{CFU}\cdot\text{mL}^{-1}$ sample shows scattered string-like aggregates in length smaller than 10 μm . Because the length of *Neisseria* is about 1 μm , there should be only three bacteria within the 3 μm focus spot via the Raman microscope objective used to acquire the spectrum. The scanning electron microscopy image showing NAEB-bound bacteria in the previous paper indicated each bacteria were bound with about 100 Raman tags [27]. Therefore, the Raman signal intensity was expected to be reproducible under this low concentration.

The other image in Fig. 3 shows densely packed *Neisseria* aggregates. Assuming each *Neisseria* was in the size of 1 $\mu\text{m} \times 0.5 \mu\text{m} \times 0.5 \mu\text{m}$, there were about 100 bacteria packed inside a cube of 3 μm . When the signal intensity is proportional to the number of bacteria, the intensity dynamic range should extend for two orders of magnitude.

These results demonstrate that NAEBs-bound bacteria at the typical concentration level of pathogen diagnosis can be trapped by the ionic wind-driven vortex flows to accumulate at the stagnant point around the center of reservoir bottom in our device. Because NAEBs contain Raman reporter molecules, their clear SERS spectrum features can confirm the specific bindings between the antibody-conjugated NAEB probes and targeted bacteria. In addition, various reporter molecules with similar scattering cross sections can be labeled in NAEBs on purpose. Therefore, the SERS signals of each type of NAEBs-bound bacteria will contain comparable intensities. When different kinds of bacteria at similar concentrations are detected simultaneously, their SERS spectrum can be easily distinguished.

Quantitation of *Neisseria*

Neisseria samples at various concentrations, 1.0×10^4 , 3.0×10^4 , 1.0×10^5 , 3.0×10^5 , and 1.0×10^6 $\text{CFU}\cdot\text{mL}^{-1}$, were mixed with a solution of NAEBs conjugated with mAb 4–7–3 antibody. An aliquot of the resulting solution (60 μL) was added into the reservoir of micro-centrifugal device. When the NAEBs-bound *Neisseria* of each sample was trapped to concentrate in 10 min or less, Raman spectrum was acquired from the bacteria accumulation spot. Figure 4 shows the peak intensities in the TRITC Raman spectra which increase proportionally with respect to the concentration of *Neisseria*. When the average peak intensity of three to five replicate

samples at 1210 cm^{-1} (I) was used to plot against bacteria concentration (C), one linear relation between the logarithm values of intensity and concentration, $\log I = 0.48 \log C + 0.14$ was found. The square correlation coefficient of this relation was 0.99. The variation of Raman signal intensities which ranged from 2% to 14% is acceptable.

The signal-to-noise (S/N) ratio of the 1210 cm^{-1} peak in the spectrum trace of 10^4 $\text{CFU}\cdot\text{mL}^{-1}$ was 13. Therefore the LOD of this method was estimated as 2300 $\text{CFU}\cdot\text{mL}^{-1}$, when S/N ratio of three was used as the criteria. This high linearity and adequate LOD indicate the feasibility of using this device to quantify bacteria at the typical concentration level for pathogen diagnosis.

Table 1 listed the comparison of nanoparticle-based methods to detect bacteria samples using various concentration devices. The figures of merit evaluations of each method are included in the table.

Immuno-microarray was used to selectively capture specific bacteria prior to conjugation with silver nanoparticles for SERS detection using the scattering signals from the functional groups on bacteria surfaces [25]. Because the inter-species signal intensity differences were usually significant using bacteria SERS spectrum, the multiplex detection capability was not versatile. Like most SERS methods, the scattering moieties were not homogeneously covered by metal nanoparticles to enhance their Raman signals. The inadequate scattering signal intensities resulted in irreproducible determinations. The reported LOD at 10^4 $\text{CFU}\cdot\text{mL}^{-1}$ was not useful either even using confocal detection.

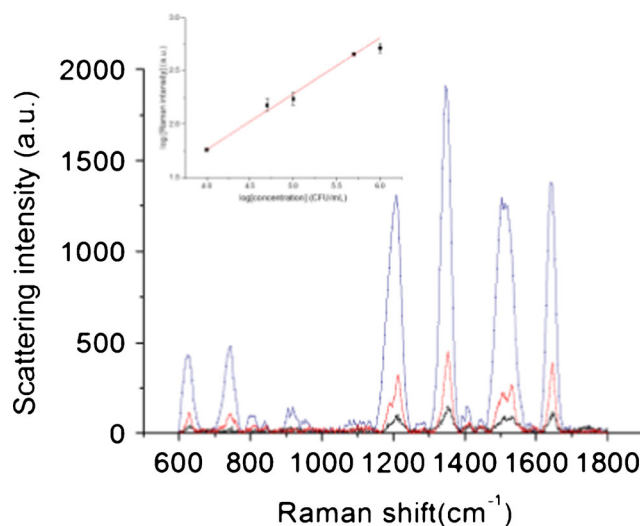


Fig. 4 The baseline corrected Raman spectrum of TRITC acquired from the concentrated NAEBs-bound *Neisseria* around the center of reservoir bottom of microcentrifugal device, where the original bacteria concentrations are 1.0×10^4 (black trace), 1.0×10^5 (red trace), and 1.0×10^6 (blue trace) $\text{CFU}\cdot\text{mL}^{-1}$, respectively. The spectrum baselines were adjusted as flat lines. The inset graph shows the linear relation between the logarithm values of intensity (I) and concentration (C), $\log I = 0.48 \log C + 0.14$, of which the square correlation coefficient is 0.99

Table 1 The comparison of nanoparticle-based methods to detect bacteria using concentration device

| Detection method | SERS [25] | SERS [30] | QD fluorescence tags [6] | SERS tags [31] | SERS tags [this work] |
|---|--|--|--------------------------|---------------------|-----------------------|
| Conc. method | Immuno- microarray | Nanorod mesh filtration | Magnetic nanoparticles | Nano-structured DEP | Micro-centrifuge |
| Sensing method | Raman spectrum features of detected bacteria | Raman spectrum features of detected bacteria | Immunoassay | Immunoassay | Immunoassay |
| Inter-species Signal intensity variations | Significant | Significant | Moderate | Moderate | Moderate |
| Selectivity | Good | Moderate | Good | Good | Good |
| Detection limit (CFU·mL ⁻¹) | 10,000 | 100 | 30 | 210 | 2300 |
| Confocal optics requirement | Yes | Yes | No | No | No |
| Multiplexity | Moderate | Moderate | Moderate | Good | Good |
| Quantitation precision | Poor | Poor | Good | Moderate | Good |
| Conc. device complexity | High | High | Low | High | Moderate |
| Conc. time (min) | 60 | 240 | 10 | 1 | 5 |

High concentration efficiency was achieved when nanorod mesh filtration was used to obtain superior LOD at 100 CFU·mL⁻¹ using confocal SERS detection [30]. However, the determination results were not reproducible. In addition, nanorod mesh fabrication required sophisticated technologies. The long filtration time of four hours also limited the convenience.

As discussed in Introduction section, functionalized magnetic nanoparticles were used to bind with bacteria for concentration prior to conjugation with QD nanoparticles for detection [6]. But the tedious assay development procedures to optimize the amounts of magnetic nanoparticles and QD nanoparticles in two incubation steps were rather time consuming. Besides, due to the broad features of fluorescence emission peaks, QD-based assays did not provide versatile multiplex detection capabilities.

In addition to this work, immunoassays using SERS tags as detection methods were carried out previously [31]. Because Raman reporter molecules were homogeneously encapsulated in gold nanoparticle clusters in the tag and each bacterium were bound with at least tens of tags, the signal reproducibility problem was therefore solved to achieve adequate quantitative detections. Both DEP and micro-centrifuge devices capture bacteria at the center of concentration reservoir to form aggregates of larger size, confocal detection is no longer required acquiring SERS signals.

Nanostructured electrode DEP concentrates bacteria more efficiently than micro-centrifuge device of this work [31]. The LOD by this DEP method was at 210 CFU·mL⁻¹ and is therefore superior to the LOD of this work at 2300 CFU·mL⁻¹. However, the device complexity of using nanostructured electrodes to provide superior sensitivity was not necessary when typical pathogen sample concentrations were at the concentration of 10³ CFU·mL⁻¹ or higher.

Adequate reporter molecules can be selected to be labeled in different tags, containing distinct Raman spectrum features. The comparable signal intensities among these tags are also adjusted. Multiplex detection to quantify several kinds of bacteria are therefore possible.

Conclusion

This work demonstrates the feasibility of using ionic wind-driven micro-centrifugal device to concentrate NAEB-bound bacteria. The Raman tags can be used to recognize and quantify bacteria at the typical level of pathogen samples, 10⁴ to 10⁶ CFU·mL⁻¹. The LOD of our method is estimated as 2300 CFU·mL⁻¹. Unlike the conventional methods that require tedious bacteria cultivation or sample preparation procedures, this method accomplishes bacteria detection within 10 min.

Although other nanoparticle-based immunoassays using impedance spectroscopy or QD fluorescence detection achieve superior LOD lower than 100 CFU·mL⁻¹, these methods are difficult to achieve multiplex detection.

Because various reporter molecules can be labeled in different tags contain distinct Raman spectrum features, this device potentially can carry out multiplex detection to simultaneously quantify several kinds of bacteria.

Acknowledgements The authors thank the grant support from the Ministry of Science and Technology, Taiwan.

Compliance with ethical standards The author(s) declare that they have no competing interests.

References

1. Dineva MA, Mahilum-Tapay L, Lee H (2007) Sample preparation: a challenge in the development of point-of-care nucleic acid-based assays for resource-limited settings. *Analyst* 132(12):1193–1199
2. Pal N, Sharma S, Gupta S (2016) Sensitive and rapid detection of pathogenic bacteria in small volumes using impedance spectroscopy technique. *Biosens Bioelectron* 77:270–277
3. Thiramanas R, Laocharoensuk R (2016) Competitive binding of polyethyleneimine-coated gold nanoparticles to enzymes and bacteria: a key mechanism for low-level colorimetric detection of gram-positive and gram-negative bacteria. *Microchim Acta* 183(1):389–396
4. Duan N, Wu S, Dai S, Miao T, Chen J, Wang Z (2015) Simultaneous detection of pathogenic bacteria using an aptamer based biosensor and dual fluorescence resonance energy transfer from quantum dots to carbon nanoparticles. *Microchim Acta* 182(5–6):917–923
5. Wang B, Wang Q, Cai Z, Ma M (2015) Simultaneous, rapid and sensitive detection of three food-borne pathogenic bacteria using multicolor quantum dot probes based on multiplex fluorimmunoassay in food samples. *LWT-Food Sci Technol* 61(2):368–376
6. Dogan Ü, Kasap E, Cetin D, Suludere Z, Boyaci IH, Türkyılmaz C, Ertas N, Tamer U (2016) Rapid detection of bacteria based on homogenous immunoassay using chitosan modified quantum dots. *Sensors Actuators B Chem* 233:369–378
7. Wu J, Ben Y, Battigelli D, Chang H-C (2005) Long-range AC electroosmotic trapping and detection of Bioparticles. *Ind Eng Chem Res* 44(8):2815–2822
8. Lui C, Cady N, Batt C (2009) Nucleic acid-based detection of bacterial pathogens using integrated microfluidic platform systems. *Sensors* 9(5):3713
9. Voldman J (2006) Electrical forces for microscale cell manipulation. *Annu Rev Biomed Eng* 8(1):425–454
10. Cheng I-F, Chen T-Y, Lu R-J, Wu H-W (2014) Rapid identification of bacteria utilizing amplified dielectrophoretic force-assisted nanoparticle-induced surface-enhanced Raman spectroscopy. *Nanoscale Res Lett* 9(1):1–8
11. Chrimes AF, Khoshmanesh K, Tang S-Y, Wood BR, Stoddart PR, Collins SSE, Mitchell A, Kalantar-zadeh K (2013) In situ SERS probing of Nano-silver coated individual yeast cells. *Biosens Bioelectron* 49:536–541
12. Cheng IF, Chang H-C, Chen T-Y, Hu C, Yang F-L (2013) Rapid (<5 min) identification of pathogen in human blood by Electrokinetic concentration and surface-enhanced Raman spectroscopy. *Sci Report* 3:2365
13. Pohl HA (1978) *Dielectrophoresis*. Cambridge University Press, London
14. Kohlheyer D, Besselink GAJ, Schlautmann S, Schasfoort RBM (2006) Free-flow zone electrophoresis and isoelectric focusing using a Microfabricated glass device with ion permeable membranes. *Lab Chip* 6(3):374–380
15. Lu H, Gaudet S, Schmidt MA, Jensen KF (2004) A Microfabricated device for subcellular organelle sorting. *Anal Chem* 76(19):5705–5712
16. Song Y-A, Chan M, Celio C, Tannenbaum SR, Wishnok JS, Han J (2010) Free-flow zone electrophoresis of peptides and proteins in PDMS microchip for narrow pI range sample Prefractionation coupled with mass spectrometry. *Anal Chem* 82(6):2317–2325
17. Kohler S, Weilbeer C, Howitz S, Becker H, Beushausen V, Belder D (2011) PDMS free-flow electrophoresis chips with integrated partitioning bars for bubble segregation. *Lab Chip* 11(2):309–314
18. Yeo LY, Hou D, Maheshwari S, Chang H-C (2006) Electrohydrodynamic surface Microvortices for mixing and particle trapping. *Appl Phys Lett* 88(23):233512
19. Hou D, Maheshwari S, Chang H-C (2007) Rapid Bioparticle concentration and detection by combining a discharge driven vortex with surface enhanced Raman scattering. *Biomicrofluidics* 1(1):014106
20. Smith E, Dent G (2013) *Modern Raman spectroscopy: a practical approach*. John Wiley & Sons, Chichester
21. Li D-W, Zhai W-L, Li Y-T, Long Y-T (2014) Recent progress in surface enhanced Raman spectroscopy for the detection of environmental pollutants. *Microchim Acta* 181(1–2):23–43
22. Krafft C, Popp J (2015) The many facets of Raman spectroscopy for biomedical analysis. *Anal Bioanal Chem* 407(3):699–717
23. Syed MA, Bokhari S (2011) Gold nanoparticle based microbial detection and identification. *J Biomed Nanotechnol* 7(2):229–237
24. Pahlow S, Meisel S, Cialla-May D, Weber K, Rösch P, Popp J (2015) Isolation and identification of bacteria by means of Raman spectroscopy. *Adv Drug Deliv Rev* 89:105–120
25. Zhou H, Yang D, Mircescu NE, Ivleva NP, Schwarzmeier K, Wieser A, Schubert S, Niessner R, Haisch C (2015) Surface-enhanced Raman scattering detection of bacteria on microarrays at single cell levels using silver nanoparticles. *Microchim Acta* 182(13–14):2259–2266
26. Huang P-J, Tay L-L, Tanha J, Ryan S, Chau L-K (2009) Single-domain antibody-conjugated nanoaggregate-embedded beads for targeted detection of pathogenic bacteria. *Chem Eur J* 15(37):9330–9334
27. Lin H-Y, Huang C-H, Hsieh W-H, Liu L-H, Lin Y-C, Chu C-C, Wang S-T, Kuo IT, Chau L-K, Yang C-Y (2014) On-line SERS detection of single bacterium using novel SERS nanoprobe and a microfluidic dielectrophoresis device. *Small* 10(22):4414–4414
28. Huang P-J, Chau L-K, Yang T-S, Tay L-L, Lin T-T (2009) Nanoaggregate-embedded beads as novel Raman labels for Biodetection. *Adv Funct Mater* 19(2):242–248
29. Tay L-L, Huang P-J, Tanha J, Ryan S, Wu X, Hulse J, Chau L-K (2012) Silica encapsulated SERS Nanoprobe conjugated to the bacteriophage Tailspike protein for targeted detection of salmonella. *Chem Commun* 48(7):1024–1026
30. Wu X, Han C, Chen J, Huang Y-W, Zhao Y (2016) Rapid detection of pathogenic bacteria from fresh produce by filtration and surface-enhanced Raman spectroscopy. *JOM* 68(4):1156–1162
31. Madiyar FR, Bhana S, Swisher LZ, Culbertson CT, Huang X, Li J (2015) Integration of a nanostructured dielectrophoretic device and a surface-enhanced Raman probe for highly sensitive rapid bacteria detection. *Nanoscale* 7(8):3726–3736